ARTICLES SCIENCE CHINA Materials

mater.scichina.com link.springer.com

Published online 17 April 2019 | https://doi.org/10.1007/s40843-019-9422-7
Sci China Mater 2019, 62(8): 1188–1198

A robust self-healing polyurethane elastomer: From H-bonds and stacking interactions to well-defined microphase morphology

Cheng-Jie Fan, Zi-Chun Huang, Bei Li, Wen-Xia Xiao, En Zheng, Ke-Ke Yang* and Yu-Zhong Wang

ABSTRACT **Self-healing materials have attracted considerable attention because of their improved safety, lifetime, energy efficiency and environmental impact. Supramolecular interactions have been extensively considered in the field of self-healing materials due to their excellent reversibility and sensitive responsiveness to environmental stimuli. However, development of a polymeric material with good mechanical performance as well as self-healing capacity is very challenging. In this study, we report a robust self-healing polyurethane (PU) elastomer polypropylene glycol-2-amino-5-(2-hydroxyethyl)-6-methylpyrimidin-4-ol (PPG-mUPy) by integrating ureidopyrimidone (UPy) motifs with a PPG segment with a well-defined architecture and microphase morphology. To balance the self-healing capacity and mechanical performance, a thermal-triggered switch of H-bonding is introduced. The quadruple H-bonded UPy dimeric moieties in the backbone induce phase separation to form a hard domain as well as enable further aggregation into microcrystals by virtue of the stacking interactions, which are stable in ambient temperature. This feature endows the PU with high mechanical strength. Meanwhile, a high healing efficiency can be realized, when the reversibility of the H-bond was unlocked from the stacking at higher temperature. An optimized sample PPG_{1000}-$mUPy^{50\%}$ with a good balance of mechanical performance (20.62 MPa of tensile strength) and healing efficiency (93% in tensile strength) was achieved. This strategy will provide a new idea for developing robust self-healing polymers.**

Keywords: polyurethane, H-bonds, stacking interaction, microphase morphology, self-healing

INTRODUCTION

The ability to spontaneously heal injuries is a key feature of biomaterials, and can improve their survivability and lifetime [1]. Inspired by nature, scientists and engineers have developed numerous self-healing materials over the past decades, especially self-healing polymers (SHPs) [2–4]. In view of the healing mechanism, all SHPs can be classified into two categories, extrinsic healing [5] and intrinsic healing mode [6,7]. The latter has attracted considerable attention owing to its repeatable self-healing capability. To realize this goal based on molecular design, all kinds of dynamic interactions have been studied by researchers. Among these, supramolecular interactions [8], such as host-guest interactions [9,10], ligand-metal complexations [11–13], π-π stacking [14–16], ionic interactions [17] and hydrogen-bonding (H-bonding) [18–20], have become the most favored choices owing to their excellent reversibility and sensitive responsiveness to environmental stimuli.

As is commonly known, H-bonding has been extensively investigated because of the rapid development of supramolecular chemistry, and a series of multiple H-bondings with high affinity and directionality were established. Ureidopyrimidone (UPy) (Scheme 1a) [21,22], which is a classic moiety developed by Meijer and can form a self-complementary quadruple H-bond with high thermodynamic stability ($\Delta G \approx 10$ kcal mol^{-1}) and rapid kinetic reversibility ($k_{off} \approx 8$ s^{-1}) [23], has been widely used to construct supramolecular self-healable materials. It has been introduced into different matrices with different topologies by employing various strategies. For example, reversible addition-fragmentation chain transfer polymerization (RAFT) was employed to prepare UPy-contained multi-block supramolecular materials [24–29]. In addition, UPy moieties could be grafted onto the polymeric backbone to obtain dynamic hydrogen-bonding

Collaborative Innovation Center for Eco-Friendly and Fire-Safety Polymeric Materials (MoE), State Key Laboratory of Polymer Materials Engineering, National Engineering Laboratory of Eco-Friendly Polymeric Materials (Sichuan), College of Chemistry, Sichuan University, Chengdu 610064, China
* Corresponding author (email: kkyangscu@126.com)

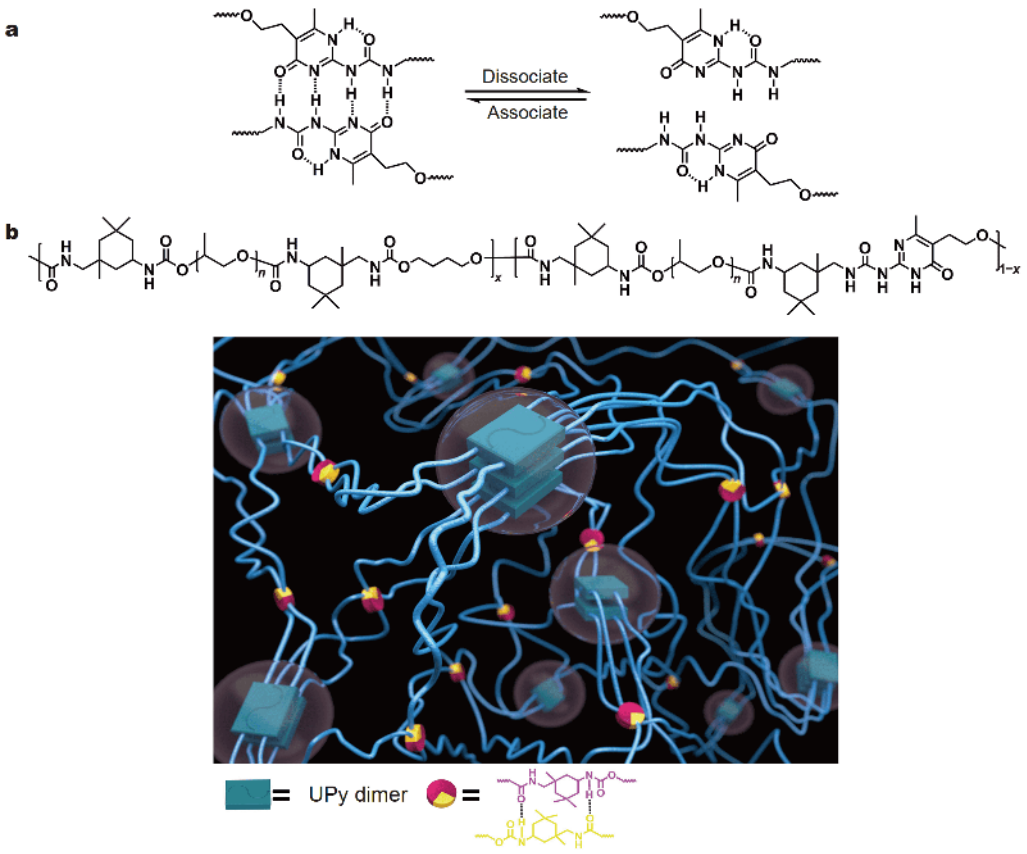

Scheme 1 (a) Schematic diagram of association and dissociation of the UPy dimer. (b) Cartoon representation of the proposed structure for PPG-mUPy.

cross-linked materials [30–33]. The UPy group has been commonly modified to the end of a small molecule [34] or polymers [35–38] in order to prepare a supramolecular cross-linking dynamic network. Actually, the excellent reversibility of UPy provides the materials with a desirable healing capacity; however, in most cases, the mechanical properties are unsatisfactory compared with systems that are derived from dynamic covalent bond.

Nowadays, an increasing number of researchers have been seeking new approaches to achieve a good balance between the mechanical performance and self-healing capacity [13,39]. A typical strategy is to tailor H-bonding array modes. Aida *et al.* [40] reported a mechanical robust and healable polymer by cross-linking low-molecular-weight polymers *via* dense H-bonds between thiourea and urea moieties, which may form a zigzag H-bonded array. Li *et al.* [41] developed a biomimetic strategy to achieve healable elastomer with supertoughness and high tensile strength by embedding hierarchical H-bonding moieties in polymer backbones. Furthermore, an effective method is to control the multiphase morphology. Guan *et al.* [25] reported a supramolecular block copolymer with a hard/soft two-phase morphology that combined high strength and toughness with spontaneous healing capability. The hard matrix of the material enables good mechanical properties; meanwhile, the reversible supramolecular moieties located within the soft phase provide self-healing capability. As is commonly known, polyurethanes (PUs) are a typical class of polymers with hard/soft two-phase morphology. PUs show great diversity in terms of both performance and morphology because they can be synthesized from various diols or polyols as well as isocyanate [42–45]. Moreover, PU architecture can be simply tuned by selecting suitable chain extenders and end-groups [46]. Taking the advantages of PU, researchers have designed many self-healing PUs containing reversible bonds (such as dynamic covalent bonds [47–52] and supramolecular interactions [53–56]). Recently, Bao *et al.* [57] developed stretchable and self-healable electronic skin or substrates for electrodes by cooperating two types of H-bonds with different bonding energies or UPy motifs in hard segments. To adapt it to the application requirements of this area, the tensile strength of these PUs is not very high

(less than 5 MPa). However, it remains challenging to develop a healable PU with high tensile strength and toughness because PUs are widely applied in the fields of light industry, engineering materials, and aerospace.

Here, to develop a robust self-healable PU elastomer with a high tensile strength and supertoughness, we propose a new strategy to achieve a good balance between the self-healing capacity and mechanical performance by the introduction of an H-bonding switch using thermal-triggered stacking interactions (Scheme 1b). For the synthetic strategy, the multiblock copolymer PPG-mUPy was prepared by coupling the flexible polypropylene glycol (PPG) diol and dynamic UPy motif with isophorone diisocyanate. Then, the supramolecular network was formed by dense quadruple H-bonds between the UPy motif in the backbone of PU chains. More important, the high content of mUPy in the backbone helps in microcrystal formation assisted by the stacking effects [58–61], which further enhances the strength of PU at ambient temperature. During stretching, the quadruple H-bonds act as sacrificial bonds to dissipate energy and provide the PU with high mechanical strength (up to 49.64 MPa) and supertoughness (up to 215.75 MJ m^{-3}). Meanwhile, this stacking structure also acts as an H-bonding switch that can be triggered by heat. When the temperature is lower than T_m of the UPy microcrystal, the reversibility of the H-bond is locked; when the temperature is higher than T_m, the dynamic nature of UPy is activated, and the excellent chain mobility of the PPG chain significantly benefits from this reassociation. By modifying the architecture and morphology of PU, an optimized sample PPG_{1000}-$mUPy^{50\%}$ with a good balance of mechanical performance and healing efficiency was declared with the excellent tensile strength of 20.62 MPa, toughness of 100.49 MJ m^{-3}, and high healing efficiency of 93% and 90%, respectively, after healing within 24 h at 80°C.

EXPERIMENTAL SECTION

Reagents and materials

PPG (AR grade, M_n=1,000, 2,000 g mol^{-1}), α-acetyl-γ-butyrolactone (99%), and guanidine carbonate (98%) were purchased from Alfa Aesar (USA). Isophorone diisocyanate (IPDI, 98%) and dibutyltin dilaurate (DBTL, 95%) were provided by Sigma-Aldrich (USA). Dimethylformamide (DMF, 99.9%) was supplied by Innochem (Beijing, China). Ethanol (AR grade), triethylamine (Et_3N, AR grade) and 1,4-butanediol (BD, AR grade) were purchased from Kelong Reagent Corp (Chengdu, China). All of the solvents and reagents were dried before use.

Synthesis of 2-amino-5-(2-hydroxyethyl)-6-methylpyrimidin-4-ol (mUPy)

mUPy was synthesized from α-acetyl-γ-butyrolactone and guanidine carbonate (Scheme S1). A detailed description of the method employed is as follows: α-acetyl-γ-butyrolactone (10.0 g, 78.1 mmol) and guanidine carbonate (14.1 g, 78.1 mmol) were added into a flask and refluxed for 12 h in absolute ethanol (100 mL) in the presence of triethylamine (26 mL) at 80°C. Then, the phases were separated, washed with ethanol and suspended in water. The mixture was neutralized using the HCl-solution. Finally, a white powder was obtained after filtrating, washing with water and ethanol, and drying.

Preparation of PPG-mUPy film

A series of PPG-mUPy with different compositions were prepared using the two-step route (Scheme S1), and the feed ratios are presented in Table S1. Taking PPG_{1000}-$mUPy^{50\%}$ as an example, the synthesis procedure was illustrated as follows. In the first step, PPG (5.00 g, 5.00 mmol) was added to a vessel and dehydrated at 80°C under vacuum for 6 h. Then, DMF (25.0 mL) was poured into the vessel as solvent under argon atmosphere. As soon as the reactants dissolved, IPDI (2.22 g, 10.00 mmol) and five drops of DBTL (about 0.06 mmol) were injected into the vessel to start the reaction. After reacting at 80°C with vigorous stirring under argon atmosphere for 2 h, NCO-terminated PU prepolymer was obtained. In the second step, without stopping the reaction, the mUPy (0.38 g, 2.25 mmol) and BD (0.21 g, 2.25 mmol) were quickly added to the mixture to extend the prepolymer chains. After reacting at 80°C for another 4 h, the solution of PPG_{1000}-$mUPy^{50\%}$ was obtained. Films with a thickness of 0.70 mm were fabricated by solution-casting from DMF at 80°C for 24 h in a horizontal Teflon dish. Finally, the film was dried in an oven at 80°C for another 12 h and transferred into a vacuum oven at 45°C for 48 h.

Characterization and measurements

Fourier transform-infrared spectrometry (FT-IR)

FT-IR spectral analysis was recorded on a Fourier transform infrared spectrometer (Nicolet 6700, USA) in a range of wavenumbers from 600 to 4,000 cm^{-1}.

Nuclear magnetic resonance (NMR) spectroscopy

NMR spectra were recorded on a Bruker AV400 spectrometer (400 MHz, Germany) with dimethyl sulfoxide-

d_6 and deuterated chloroform as solutions and tetramethyl silane (TMS) as the internal reference.

Gel permeation chromatography (GPC)
GPC was carried out with the HLC-8320 system (Tosoh Corporation, Japan) equipped with a refractive index detector and two columns, two TSK gel super AWM-H. DMF acted as elution solvent with a flow rate of 0.4 mL min^{-1} at 35°C and a polymethylmethacrylate (PMMA) standard was used for calibration.

Small-angle X-ray scattering (SAXS)
SAXS experiments were implemented on the Xeuss 2.0 system (Xenoc, France). A multilayer focused Cu Kα X-ray source (GeniX3D Cu ULD, Xenocs SA, France, λ= 0.154 nm) and scatterless collimating slits were used during the measurements. The value of periodic length d was calculated by formula $d=2\pi/q$.

Differential scanning calorimetry (DSC)
DSC was performed with a DSC-Q200 (TA Instrument, USA) over the temperature range from −70 to 140°C at a heating (or cooling) rate of 3°C min^{-1} under a steady flow of ultra-high-purity nitrogen purge and empty aluminum as the reference.

Dynamic mechanical analysis (DMA)
The dynamic mechanical analysis of the samples was investigated using DMA Q800 (TA Instruments, USA), with a heating rate of 3°C min^{-1} from −60 to 150°C, and at a frequency of 1 Hz.

Static tensile tests
The mechanical properties of the samples were investigated on an Instron Universal Testing Machine (Model 3366, Instron Crop, USA) at a loading speed of 100 mm min^{-1} at room temperature. The thickness and width of the specimens were 0.70 and 4 mm, respectively. And the length of the sample between the two pneumatic grips of the testing machine was 20 mm. Five dumbbell-shaped specimens were tested in each sample.

Self-healing test
To qualitatively analyze self-healing performance of the PPG-mUPy, the samples were firstly damaged with a razor blade to create a crack about 20 μm in width on the surface. Then, an optical microscope (Nikon DA-Fi1, Japan) was used to observe the sample surface before and after healing. The quantitative self-healing performance of the prepared samples was determined by healing efficiencies (see details in Equation S1) which were calculated from tensile test (using the Instron Universal Testing Machine). The dumbbell-shaped specimens were cut into two completely separate using a razor blade. Immediately after, the two separate halves were brought into contact with suitably applied stress in one minute. Then the samples were put into the oven at a controlled condition. After that, all specimens were tested by Instron Universal Testing Machine with a loading speed of 100 mm min^{-1} at room temperature.

RESULTS AND DISCUSSION

Preparation of PPG-mUPy
To embed the UPy moieties into the PPG main chains, a functionalized monomer mUPy comprising a hydroxyl group and an amidogen group was first prepared, and the synthetic strategy of mUPy is illustrated (Scheme S1) and its chemical structure is confirmed using an ^{1}H NMR spectrum (Fig. S1). Meanwhile, the OCN-PPG-NCO was prepared by decorating the NCO group onto the chain-end of the PPG diol. Then, the target PU, which was referred to as PPG_x-$mUPy^y$, was prepared by coupling OCN-PPG-NCO with equivalent mUPy and BD (Scheme S1), where the subscript x is the molecular weight of PPG, and the superscript y is the mole fraction of mUPy. The reaction of the chain extension was monitored by FT-IR based on the decline of the characteristic peak of the NCO group (Fig. S2). Finally, the molecular features of the target products were determined by ^{1}H NMR (Fig. S3) and GPC analysis (all data were listed in Table S1).

Characterization of the quadruple H-bonding
In this work, the quadruple H-bond formed by UPy dimerization was the driven force to construct a supramolecular polyurethane network. As is previously known, UPy groups could associate and disassociate under suitable conditions, as illustrated in Scheme 1a. To identify this feature, ^{1}H NMR analysis was first conducted in different solvents. As shown in Fig. S4 in the Supplementary information, the characteristic peaks of N–H in UPy unites appeared at 12.92 ppm (δ_{H^a}), 11.95 ppm (δ_{H^b}), and 10.09 ppm (δ_{H^c}) in $CDCl_3$, and these peaks were found to shift to a high field at 11.37 ppm (δ_{H^a}), 9.31 ppm (δ_{H^b}), and 7.71 ppm (δ_{H^c}) in DMSO-d_6, respectively. This is because of the high self-association constant of UPy dimer in chloroform ($K_{dim}\geq10^7$ L mol^{-1}), and the UPy existed as a mixture of the pyrimidin-4-ol and the 4[1*H*]-pyrimidinone. However, the UPy existed as the 6[1*H*]-pyrimidinone form in DMSO-d_6, which could not form

dimers [21–23].

Thermal behavior and micromorphology of PPG-mUPy samples

From the perspective of the molecular design in current systems, the micromorphology of the PPG-mUPy plays a dominant role in its mechanical properties and self-healing capacity. Hence, DSC and SAXS were employed to disclose the relationship between the molecular structure and the micromorphology. Fig. 1a shows the DSC curves of the PPG-based samples in the heating scan. The relevant thermal parameters and their corresponding values are listed in Table S2. Two main factors were found to affect the thermal behaviors of PU. One is the molecular weight of the PPG precursor, and the other is the content of mUPy. Compared with the PPG_{1000}-mUPy series, the sample PPG_{2000}-$mUPy^{100\%}$ with a longer chain length of soft segment exhibits a lower glass-transition temperature (T_g) at −57°C. Meanwhile, it is expected that the T_g shows an increasing tendency with the increase of mUPy, because the formation of a greater number of quadruple H-bonds will restrict the mobility of polymer chains. Further, we also found that PPG-mUPy displayed a broad endothermic peak around 77°C during the heating process, which may be attributed to the melt of the UPy microcrystal. To confirm this viewpoint, PPG_{1000}-$BD^{100\%}$, which is a blank sample without mUPy, was also analyzed using DSC (Fig. 1a, Table S2). As was expected, there was no endothermic peak above T_g, which indicated that this sample was in the amorphous state. As reported in some other systems that contained UPy moieties [59–62], the π-π stacking interaction of the UPy structure and the H-bonding of carbamate groups could actually induce the UPy dimer to form microcrystals. Therefore, it is easy to understand that the relevant enthalpy ΔH_m of PPG-mUPy increases with the increase of the proportion of mUPy (Table S2). For the samples with a similar mUPy content, e.g., PPG_{2000}-$mUPy^{100\%}$ and PPG_{1000}-$mUPy^{50\%}$, the latter possesses higher ΔH_m, which may be explained as being caused by the higher density of H-bonding of the carbamate groups stabilizing the stacking of UPy moieties.

After the formation of the UPy crystal was proven by performing the DSC test, SAXS was carried out to analyze the microstructure of the materials (Fig. 1b and Fig. S5). The SAXS profiles indicated that PPG-mUPy samples had a long period peak at q=0.15 A^{-1}, corresponding to a d spacing of 4.19 nm. This indicated the presence of a phase separation between the hard and soft segments because of the stacking of UPy dimers. Then, the intensities of the peaks were enhanced by increasing the mUPy content. On the contrary, no obvious peak was found in the blank sample PPG_{1000}-$BD^{100\%}$. Up until the present, as was expected, the microphase separation in the PPG-mUPy was demonstrated. Hereafter, the mechanical properties and self-healing behavior are explored systematically.

Static tensile properties and self-healing performance of PPG-based samples

Fig. 2a displays the stress-strain curves for the PPG-based samples, and the mechanical properties are summarized in Table 1. These curves of PPG-mUPy are relatively linear with deforming, and there is no yield-like component, which presents a classical rubberlike behavior. Compared with the UPy-free sample PPG_{1000}-$BD^{100\%}$, which exhibits very poor mechanical performance with a tensile strength about 0.05 MPa and a toughness of 0.15 MJ m^{-3}, the mechanical properties of the PPG-mUPy samples were significantly enhanced owing to the presence of the quadruple H-bonding and the UPy microcrystal. It is clear that the content of the mUPy group as well as the density of the H-bonding influences the me-

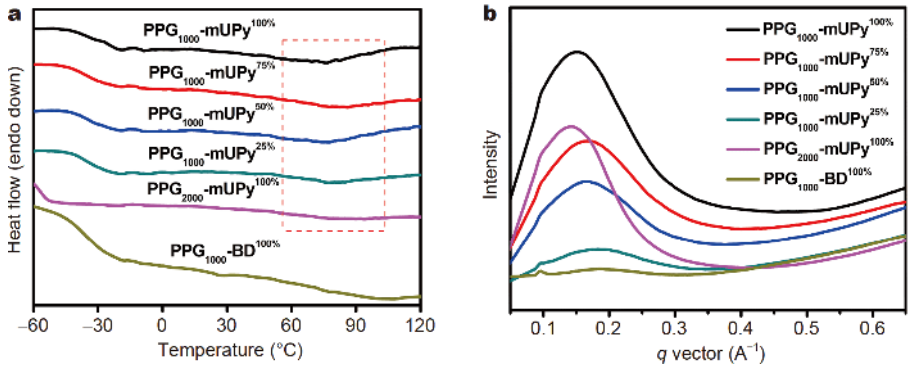

Figure 1 (a) DSC curves of PPG-based samples: heating run at a rate of 3°C min^{-1}. (b) SAXS data for PPG-based samples recorded at 25°C.

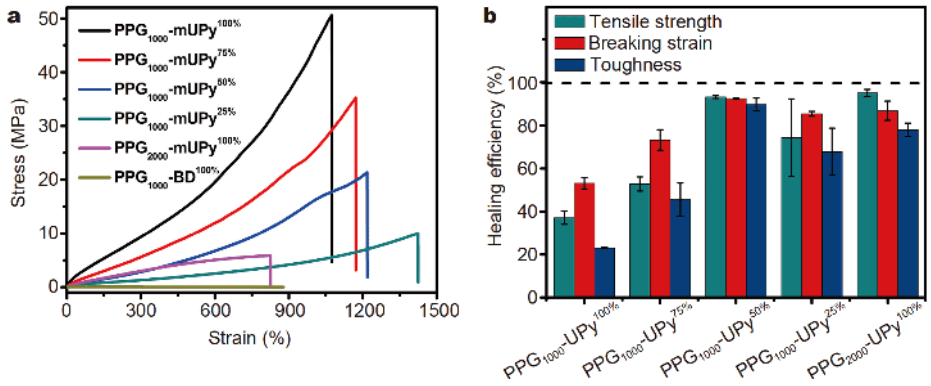

Figure 2 (a) Stress-strain curves obtained from static tensile tests. (b) The healing was conducted at 80°C for 24 h, while the healing efficiency was determined from the tensile properties of the healed specimens at 25°C.

Table 1 Summary of mechanical properties of PPG-based samples (measured at a stretching speed of 100 mm min^{-1})

Samples	Tensile strength (MPa)	Strain at break (%)	Young's modulus (MPa)	Toughness (MJ m^{-3})
PPG_{1000}-$mUPy^{100\%}$	49.64±3.54	1070±7	7.82±1.28	215.73±8.89
PPG_{1000}-$mUPy^{75\%}$	36.31±1.53	1129±61	6.48±1.00	154.93±5.75
PPG_{1000}-$mUPy^{50\%}$	20.62±1.06	1232±19	2.59±0.43	100.49±2.21
PPG_{1000}-$mUPy^{25\%}$	9.62±0.62	1512±166	1.29±0.12	53.54±7.32
PPG_{2000}-$mUPy^{100\%}$	5.91±0.08	825±37	1.04±0.03	30.61±2.42
PPG_{1000}-$BD^{100\%}$	0.05±0.01	798±146	0.25±0.03	0.12±0.03

chanical property greatly. For the PPG_{1000}-mUPy series, the tensile strength (σ) and toughness of supramolecular networks were gradually decreased from 49.64 MPa/215.73 MJ m^{-3} to 9.62 MPa/53.54 MJ m^{-3}, when the mUPy content varied from 100% to 25%; meanwhile, the elongation at the break (ε) increased slightly from 1,070% to 1,512% because the flexibility of the polymer chains increased. In fact, not only the H-bonds formed by UPy groups contribute to the mechanical performance, but the H-bonds formed by the carbamate group also benefit the mechanical performance in our current system. Therefore, the PPG_{2000}-$mUPy^{100\%}$ sample showed a lower mechanical strength than PPG_{1000}-$mUPy^{50\%}$ with a similar mUPy content. Considering these two factors, it is easy to understand that PPG_{1000}-$mUPy^{100\%}$ exhibited the maximum tensile strength and supertoughness.

In the present work, the dynamic nature of the H-bonding and the good mobility of the soft PPG segment in the samples could provide PPG-mUPy samples with the desirable self-healing capability. To reveal this feature, qualitative and quantitative analyses were conducted by performing optical microscopy and tensile tests, respectively.

As mentioned above, the UPy groups in the main chain could form a crystal and melt at around 77°C. Thus, taking PPG_{1000}-$mUPy^{50\%}$ as an example, we chose two typical temperatures (below and above 77°C) to observe its self-healing behavior using optical microscopy. At 70°C, a poor performance was observed (Fig. S6a), which may be attributed to the lower chain mobility caused by the stacking structure of the UPy microcrystal. However, at 80°C, the scratch on the film almost completely disappeared after healing for 6 h (Fig. 3a), indicating a good self-healing ability at this temperature. This result shows that the H-bonds of UPy moieties and carbamate groups could quickly reassociate between the interfaces (Fig. 3b) at this temperature. In addition, the facilitation of the dynamic feature of H-bonding and the ease of diffusion of the flexible PPG segment to repair the mechanical properties of the sample are present at the macro level (Fig. 3c, video in the Supplementary information). When the temperature was higher than 80°C, the scratch on the film could disappear completely within a shorter time (Fig. S6b, c).

The tensile tests of the samples before being damaged and after healing were conducted to quantitatively ana-

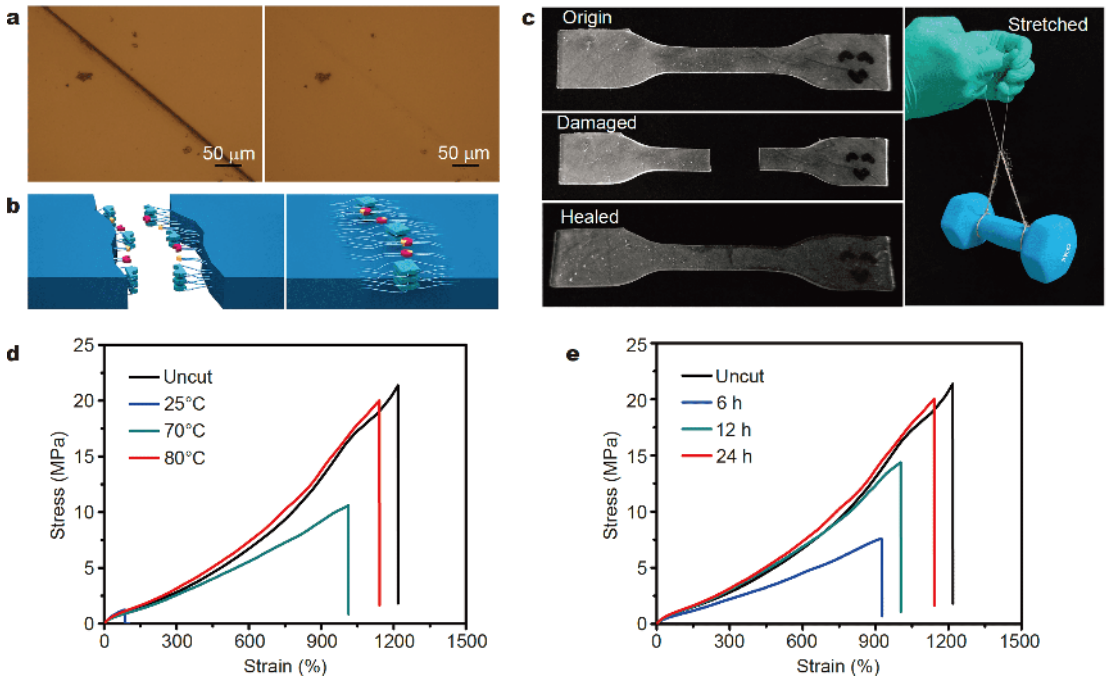

Figure 3 Self-healing performance tests. (a) Optical micrographs of the PPG_{1000}-$mUPy^{50\%}$ damaged and healed at 80°C for 6 h. (b) Schematic mechanism for the self-healing process of PPG-mUPy samples. (c) Photographs of PPG_{1000}-$mUPy^{50\%}$ (length: 50 mm, width: 4 mm, thickness: 0.7 mm) origin, damaged, healed at (80°C for 24 h) and stretched after healed (with a 3 kg dumbbell). (d) The stress–strain curves for PPG_{1000}-$mUPy^{50\%}$ in the original state and healed at different temperatures for 24 h. (e) The stress-strain curves for PPG_{1000}-$mUPy^{50\%}$ in original state and healed at 80°C for different times.

lyze the self-healing properties. In more detail, the dog-bone-shaped PPG-mUPy samples were cut into two pieces with a razor, and then the two pieces were gently pressed for 1 min, and then put into an oven for 24 h at 80°C; for comparison, the original samples were treated with the same thermal history. The stress-strain curves of PPG-mUPy samples before being damaged and after healing under different conditions are shown (Fig. 3d, e and Fig. S7). The self-healing efficiency (η) was calculated from the ratio of the mechanical properties of the healed and the original samples (Equation S1), and the impact of the material structure on η is illustrated in Fig. 2b. For the PPG_{1000}-mUPy series, the η increased first and then decreased, while the mUPy content decreased. Actually, there are two factors that influence the self-healing ability in this system, the polymeric chain mobility and the density of the H-bonding. The sample with high mUPy content has a high density of H-bonding, but the mobility of PPG chains has been restricted. Here, the PPG_{1000}-$mUPy^{50\%}$ shows a good balance between these two factors, and it exhibits the best healing capacity. After healing, σ of the sample has recovered to 19.22 MPa with an η_σ value of 93%. Then, based on this sample, the influence of the healing temperature and time on η was investigated. Fig. 3d, e illustrate the stress-strain curves of PPG_{1000}-$mUPy^{50\%}$ healed at different temperatures (Fig. 3d, Fig. S8) and different times (Fig. 3e), respectively. The figures show that increasing the healing temperature or prolonging the healing time will be advantageous to the healing of cracks. On one hand, a suitable temperature could provide a sufficient mobility of the polymeric chain, as mentioned above. On the other hand, prolonging the time allows a full chain diffusion at the section interface, which is considered as the primary driving force for healing, until the diffusion reaches the equilibrium state. For PPG_{1000}-$mUPy^{50\%}$, after healing for 12 h, the recovery of σ and ε reached 70% and 82%, respectively. A further increase in the healing time to 24 h led η_σ to improve to 93%, while η_ε increased to 93%, which almost approached the original level.

Dynamic feature of quadruple H-bonding

In order to better understand the mutual effect between the dynamic feature of H-bonding and the chain viscoelastic behaviors, DMA and cyclic tensile tests were performed. First, the storage modulus (E') and the loss factor (tanδ) of the PPG-based samples as a function of temperature were recorded by DMA (Fig. 4a). In Fig. 4a, all

of the samples exhibit a marked decrease of E' when the temperature exceeds the T_g. More evidently, the transition is displayed as a peak in the tanδ curves, and the values of T_g obtained by the curves are presented in Table S3. Although the T_g determined by DMA is higher than what is recorded by DSC, it shows the same variation trend. It should be noted that when the temperature exceeded T_g, a platform appeared in the samples with UPy moieties owing to the presence of the supramolecular network stabilized by H-bonding between UPy and their microcrystals. Not surprisingly, the sample with the high mUPy content possessed a higher E' value, which is consistent with the results of the tensile test previously discussed in this paper. When the temperature further increased above T_m, there was another visible decline of E', because the UPy crystal was molten and the quadruple H-bonding was gradually broken up. For comparison, the PPG_{1000}-$BD^{100\%}$ sample with no UPy moiety showed the lowest E' value, and it was collapsed at around 60°C.

To further explore the dynamic behavior of H-bonding, the stress-relaxation measurements were conducted by stretching the PPG-mUPy samples to 50% strain at 80°C and maintaining the strain for 60 min (Fig. 4b). Obviously, all PPG-mUPy samples undergo stress relaxation within 60 min, and just the relaxation rate of PPG_{1000}-mUPy samples largely depends on the density of the H-bonds as well as the mUPy content. PPG_{1000}-$mUPy^{100\%}$ with the highest mUPy content showed the lowest relaxation rate, and it maintained the highest residual stress about 13.57% at 60 min; on the contrary, PPG_{1000}-$mUPy^{25\%}$ showed the highest relaxation rate, and a stress of only 0.04% was maintained at the same stress relaxation time. Thus, it is easy to understand that PPG_{1000}-$mUPy^{50\%}$ and PPG_{2000}-$mUPy^{100\%}$, which possess almost the same mUPy content, displayed the similar residual stress of 2.10% and 2.09% after the same stress relaxation time, respectively. The dissociation and association of quadruple H-bonds constantly occur in the stretched PPG-mUPy samples, thus allowing the network topologies of the PPG-mUPy samples to adapt to the applied forces. Therefore, this dynamic nature of the quadruple H-bonded crosslinking network at 80°C provides the self-healing ability of the PPG-mUPy samples.

Moreover, the cyclic tensile tests were also performed

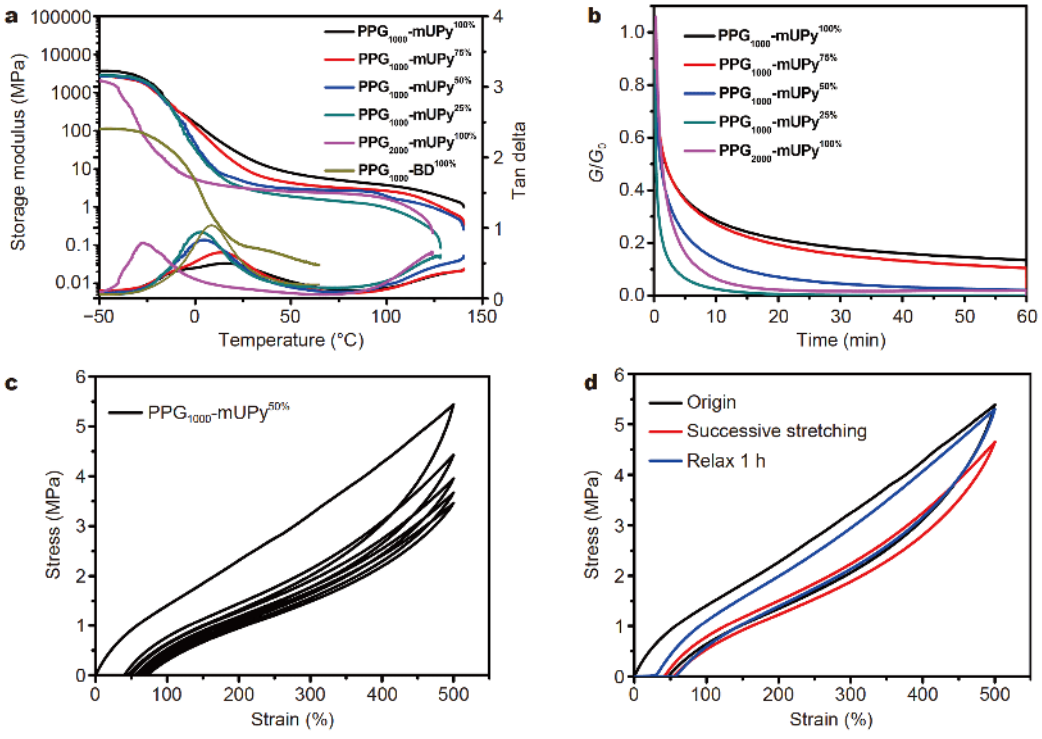

Figure 4 (a) Storage modulus curves (E') and the loss factor (tanδ) curves recorded from DMA tests. (b) Stress relaxation curves of PPG-mUPy samples. The samples were stretched to a strain of 50% at 80°C and then maintained for 60 min to record the stress relaxation data. (c) Cyclic stress-strain curve (up to 500% strain with five circles) of PPG_{1000}-$mUPy^{50\%}$ polymer film. (d) Cyclic stress-strain curve of PPG_{1000}-$mUPy^{50\%}$ polymer film (up to 500% strain) at first loading (black), second loading (red) successively and third loading (blue) after 1 h rest, respectively.

to reveal the dynamic nature of H-bonding in the present system from the perspective of the energy dissipation. First, PPG-mUPy samples were successively loaded-unloaded for five cycles at 500% strain (Fig. 4c and Fig. S9). The PPG_{1000}-$mUPy^{50\%}$ sample was observed to have a significant hysteresis (4.75 MJ m^{-3} for 500% strain cycle) and excellent elastic recovery rates (~90% for 500% strain cycle) in the first loading-unloading cycle. In the subsequent second cycle, the loading-unloading curve is closer to the previous unloading curves with relatively small hysteresis (1.49 MJ m^{-3} for a 500% strain cycle). It shows the typical Mullins effect, i.e., stress softening behavior because of hysteresis effects resulting from the disruption of the microstructure, dissociation of H-bonds, orientation of the hard segment domains, etc. [62–65]. The subsequent cycles exhibit the same phenomenon. Then, taking PPG_{1000}-$mUPy^{50\%}$ as an example, a comparative test was conducted: first, the samples were successively loaded-unloaded for two cycles at 500% strain; then, the third cycle of loading-unloading at 500% strain proceeded after 1 h relaxation (Fig. 4d). Compared with the second cycle with distinct hysteresis, the sample almost recovered its stress-strain property in the third cycle after 1 h relaxation because the disassociated H-bonds during the stretch in the previous cycle was associated after a period of time. This could be further proof of the dynamic feature of the quadruple H-bonding. Meanwhile, the loading-unloading curves had remarkable repeatability when the strain was below 200%, which indicates the quick recovery at the low strain, and as shown in Fig. S10.

CONCLUSIONS

In summary, a series of PPG-mUPy supramolecular PU elastomers were successfully prepared on the coupling PPG diol and mUPy with isophorone diisocyanate. DSC and SAXS analyses reveal that the dense UPy dimeric moieties in the PU backbone may self-assemble to stacks and induce microphase separation. The well-defined microphase structure with a strong and stable hard domain matched with a highly flexible PPG soft domain results in PU with high strength and supertoughness; meanwhile, the dynamic nature of H-bonding provides the supramolecular network with a desirable self-healing capacity. The impact of the PPG segment length, composition and the microphase morphology on the performance were investigated, and PPG_{1000}-$mUPy^{50\%}$ was found to be as an optimized sample with a good balance of mechanical performance (20.62 MPa of tensile strength and 100.49 MJ m^{-3} of toughness) and healing efficiency (93% in tensile strength and 93% in toughness after healing within 24 h at 80°C).

Received 24 January 2019; accepted 25 March 2019; published online 17 April 2019

1 Diesendruck CE, Sottos NR, Moore JS, *et al.* Biomimetic self-healing. Angew Chem Int Ed, 2015, 54: 10428–10447
2 An SY, Arunbabu D, Noh SM, *et al.* Recent strategies to develop self-healable crosslinked polymeric networks. Chem Commun, 2015, 51: 13058–13070
3 Wei Z, Yang JH, Zhou J, *et al.* Self-healing gels based on constitutional dynamic chemistry and their potential applications. Chem Soc Rev, 2014, 43: 8114–8131
4 Yang Y, Urban MW. Self-healing polymeric materials. Chem Soc Rev, 2013, 42: 7446
5 White SR, Sottos NR, Geubelle PH, *et al.* Autonomic healing of polymer composites. Nature, 2001, 409: 794–797
6 Hart LR, Harries JL, Greenland BW, *et al.* Healable supramolecular polymers. Polym Chem, 2013, 4: 4860
7 Roy N, Bruchmann B, Lehn JM. Dynamers: Dynamic polymers as self-healing materials. Chem Soc Rev, 2015, 44: 3786–3807
8 Campanella A, Döhler D, Binder WH. Self-healing in supramolecular polymers. Macromol Rapid Commun, 2018, 39: 1700739
9 Liu J, Scherman OA. Cucurbit[*n*]uril supramolecular hydrogel networks as tough and healable adhesives. Adv Funct Mater, 2018, 28: 1800848
10 Peng L, Zhang H, Feng A, *et al.* Electrochemical redox responsive supramolecular self-healing hydrogels based on host–guest interaction. Polym Chem, 2015, 6: 3652–3659
11 Du L, Xu ZY, Fan CJ, *et al.* A fascinating metallo-supramolecular polymer network with thermal/magnetic/light-responsive shape-memory effects anchored by Fe_3O_4 nanoparticles. Macromolecules, 2018, 51: 705–715
12 Tang L, Chen X, Wang L, *et al.* Metallo-supramolecular hydrogels based on amphiphilic polymers bearing a hydrophobic schiff base ligand with rapid self-healing and multi-stimuli responsive properties. Polym Chem, 2017, 8: 4680–4687
13 Zheng Q, Ma Z, Gong S. Multi-stimuli-responsive self-healing metallo-supramolecular polymer nanocomposites. J Mater Chem A, 2016, 4: 3324–3334
14 Burattini S, Greenland BW, Merino DH, *et al.* A healable supramolecular polymer blend based on aromatic π–π stacking and hydrogen-bonding interactions. J Am Chem Soc, 2010, 132: 12051–12058
15 Burattini S, Colquhoun HM, Fox JD, *et al.* A self-repairing, supramolecular polymer system: healability as a consequence of donor–acceptor π–π stacking interactions. Chem Commun, 2009, 319: 6717
16 Mei JF, Jia XY, Lai JC, *et al.* A highly stretchable and autonomous self-healing polymer based on combination of Pt···Pt and π-π interactions. Macromol Rapid Commun, 2016, 37: 1667–1675
17 Das A, Sallat A, Böhme F, *et al.* Ionic modification turns commercial rubber into a self-healing material. ACS Appl Mater Interfaces, 2015, 7: 20623–20630
18 Cao J, Lu C, Zhuang J, *et al.* Multiple hydrogen bonding enables the self-healing of sensors for human-machine interactions. Angew Chem Int Ed, 2017, 56: 8795–8800
19 Cao PF, Li B, Hong T, *et al.* Superstretchable, self-healing poly-

meric elastomers with tunable properties. Adv Funct Mater, 2018, 28: 1800741
20 Kang J, Son D, Wang GJN, *et al.* Tough and water-insensitive self-healing elastomer for robust electronic skin. Adv Mater, 2018, 30: 1706846
21 Beijer FH, Sijbesma RP, Kooijman H, *et al.* Strong dimerization of ureidopyrimidones *via* quadruple hydrogen bonding. J Am Chem Soc, 1998, 120: 6761–6769
22 Beijer FH, Kooijman H, Spek AL, *et al.* Self-complementarity achieved through quadruple hydrogen bonding. Angew Chem Int Ed, 1998, 37: 75–78
23 Söntjens SHM, Sijbesma RP, van Genderen MHP, *et al.* Stability and lifetime of quadruply hydrogen bonded 2-ureido-4[1*H*]-pyrimidinone dimers. J Am Chem Soc, 2000, 122: 7487–7493
24 Cui J, del Campo A. Multivalent H-bonds for self-healing hydrogels. Chem Commun, 2012, 48: 9302
25 Hentschel J, Kushner AM, Ziller J, *et al.* Self-healing supramolecular block copolymers. Angew Chem Int Ed, 2012, 51: 10561–10565
26 Faghihnejad A, Feldman KE, Yu J, *et al.* Adhesion and surface interactions of a self-healing polymer with multiple hydrogen-bonding groups. Adv Funct Mater, 2014, 24: 2322–2333
27 Zhu D, Ye Q, Lu X, *et al.* Self-healing polymers with PEG oligomer side chains based on multiple H-bonding and adhesion properties. Polym Chem, 2015, 6: 5086–5092
28 Foster EM, Lensmeyer EE, Zhang B, *et al.* Effect of polymer network architecture, enhancing soft materials using orthogonal dynamic bonds in an interpenetrating network. ACS Macro Lett, 2017, 6: 495–499
29 van Gemert GML, Peeters JW, Söntjens SHM, *et al.* Self-healing supramolecular polymers in action. Macromol Chem Phys, 2012, 213: 234–242
30 Chirila TV, Lee HH, Oddon M, *et al.* Hydrogen-bonded supramolecular polymers as self-healing hydrogels: Effect of a bulky adamantyl substituent in the ureido-pyrimidinone monomer. J Appl Polym Sci, 2014, 131: 39932
31 Zhang G, Lv L, Deng Y, *et al.* Self-healing gelatin hydrogels cross-linked by combining multiple hydrogen bonding and ionic coordination. Macromol Rapid Commun, 2017, 38: 1700018
32 Wu Y, Wang L, Zhao X, *et al.* Self-healing supramolecular bioelastomers with shape memory property as a multifunctional platform for biomedical applications *via* modular assembly. Biomaterials, 2016, 104: 18–31
33 Chen S, Bi X, Sun L, *et al.* Poly(sebacoyl diglyceride) cross-linked by dynamic hydrogen bonds: A self-healing and functionalizable thermoplastic bioelastomer. ACS Appl Mater Interfaces, 2016, 8: 20591–20599
34 Balkenende DWR, Monnier CA, Fiore GL, *et al.* Optically responsive supramolecular polymer glasses. Nat Commun, 2016, 7: 10995
35 Oya N, Ikezaki T, Yoshie N. A crystalline supramolecular polymer with self-healing capability at room temperature. Polym J, 2013, 45: 955–961
36 Wei M, Zhan M, Yu D, *et al.* Novel poly(tetramethylene ether) glycol and poly(ε-caprolactone) based dynamic network *via* quadruple hydrogen bonding with triple-shape effect and self-healing capacity. ACS Appl Mater Interfaces, 2015, 7: 2585–2596
37 Sautaux J, Montero de Espinosa L, Balog S, *et al.* Multistimuli, multiresponsive fully supramolecular orthogonally bound polymer networks. Macromolecules, 2018, 51: 5867–5874
38 Liu M, Liu P, Lu G, *et al.* Multiphase-assembly of siloxane oligomers with improved mechanical strength and water-enhanced healing. Angew Chem Int Ed, 2018, 57: 11242–11246
39 Liu J, Liu J, Wang S, *et al.* An advanced elastomer with an unprecedented combination of excellent mechanical properties and high self-healing capability. J Mater Chem A, 2017, 5: 25660–25671
40 Yanagisawa Y, Nan Y, Okuro K, *et al.* Mechanically robust, readily repairable polymers *via* tailored noncovalent cross-linking. Science, 2018, 359: 72–76
41 Song Y, Liu Y, Qi T, *et al.* Towards dynamic but supertough healable polymers through biomimetic hierarchical hydrogen-bonding interactions. Angew Chem Int Ed, 2018, 57: 13838–13842
42 Zhan MQ, Yang KK, Wang YZ. Shape-memory poly(*p*-dioxanone)–poly(ε-caprolactone)/sepiolite nanocomposites with enhanced recovery stress. Chin Chem Lett, 2015, 26: 1221–1224
43 Xie H, Cheng CY, Du L, *et al.* A facile strategy to construct PDLLA-PTMEG network with triple-shape effect *via* photo-cross-linking of anthracene groups. Macromolecules, 2016, 49: 3845–3855
44 He MJ, Xiao WX, Xie H, *et al.* Facile fabrication of ternary nanocomposites with selective dispersion of multi-walled carbon nanotubes to access multi-stimuli-responsive shape-memory effects. Mater Chem Front, 2017, 1: 343–353
45 Deng XY, Xie H, Du L, *et al.* Polyurethane networks based on disulfide bonds: From tunable multi-shape memory effects to simultaneous self-healing. Sci China Mater, 2019, 62: 437–447
46 Kim SM, Jeon H, Shin SH, *et al.* Superior toughness and fast self-healing at room temperature engineered by transparent elastomers. Adv Mater, 2018, 30: 1705145
47 Martin R, Rekondo A, Ruiz de Luzuriaga A, *et al.* The processability of a poly(urea-urethane) elastomer reversibly crosslinked with aromatic disulfide bridges. J Mater Chem A, 2014, 2: 5710
48 Rivero G, Nguyen LTT, Hillewaere XKD, *et al.* One-pot thermoremendable shape memory polyurethanes. Macromolecules, 2014, 47: 2010–2018
49 Heo Y, Sodano HA. Self-healing polyurethanes with shape recovery. Adv Funct Mater, 2014, 24: 5261–5268
50 Zhang ZP, Rong MZ, Zhang MQ. Mechanically robust, self-healable, and highly stretchable "living" crosslinked polyurethane based on a reversible CC bond. Adv Funct Mater, 2018, 28: 1706050
51 Ji SB, Cao W, Yu Y, *et al.* Visible-light-induced self-healing diselenide-containing polyurethane elastomer. Adv Mater, 2015, 27: 7740–7745
52 Zhang Y, Ying H, Hart KR, *et al.* Malleable and recyclable poly (urea-urethane) thermosets bearing hindered urea bonds. Adv Mater, 2016, 28: 7646–7651
53 Wu X, Wang J, Huang J, *et al.* Robust, stretchable, and self-healable supramolecular elastomers synergistically cross-linked by hydrogen bonds and coordination bonds. ACS Appl Mater Interfaces, 2019, 11: 7387–7396
54 Pan Y, Hu J, Yang Z, *et al.* From fragile plastic to room-temperature self-healing elastomer: Tuning quadruple hydrogen bonding interaction through one-pot synthesis. ACS Appl Polym Mater, 2019, 1: 425–436
55 Hong G, Zhang H, Lin Y, *et al.* Mechanoresponsive healable metallosupramolecular polymers. Macromolecules, 2013, 46: 8649–8656
56 Feula A, Pethybridge A, Giannakopoulos I, *et al.* A thermoreversible supramolecular polyurethane with excellent healing

ability at 45 degrees C. Macromolecules, 2015, 48: 6132–6141
57 Yan X, Liu Z, Zhang Q, *et al.* Quadruple H-bonding cross-linked supramolecular polymeric materials as substrates for stretchable, antitearing, and self-healable thin film electrodes. J Am Chem Soc, 2018, 140: 5280–5289
58 Söntjens SHM, Renken RAE, van Gemert GML, *et al.* Thermoplastic elastomers based on strong and well-defined hydrogen-bonding interactions. Macromolecules, 2008, 41: 5703–5708
59 Fang X, Zhang H, Chen Y, *et al.* Biomimetic modular polymer with tough and stress sensing properties. Macromolecules, 2013, 46: 6566–6574
60 Appel WPJ, Portale G, Wisse E, *et al.* Aggregation of ureido-pyrimidinone supramolecular thermoplastic elastomers into nanofibers: A kinetic analysis. Macromolecules, 2011, 44: 6776–6784
61 Teunissen AJP, Nieuwenhuizen MML, Rodríguez-Llansola F, *et al.* Mechanically induced gelation of a kinetically trapped supramolecular polymer. Macromolecules, 2014, 47: 8429–8436
62 Lee K, Lee B, Kim C, *et al.* Stress-strain behavior of the electrospun thermoplastic polyurethane elastomer fiber mats. Macromol Res, 2005, 13: 441–445
63 Qi HJ, Boyce MC. Stress–strain behavior of thermoplastic polyurethanes. Mech Mater, 2005, 37: 817–839
64 Buckley CP, Prisacariu C, Martin C. Elasticity and inelasticity of thermoplastic polyurethane elastomers: Sensitivity to chemical and physical structure. Polymer, 2010, 51: 3213–3224
65 Fu D, Pu W, Wang Z, *et al.* A facile dynamic crosslinked healable poly(oxime-urethane) elastomer with high elastic recovery and recyclability. J Mater Chem A, 2018, 6: 18154–18164

Acknowledgements This work was financially supported by the National Natural Science Foundation of China (51773131, 51811530149 and 51721091) and the International S&T Cooperation Project of Sichuan Province (2017HH0034).

Author contributions Fan CJ designed the structure, performed the experiments, analyzed the data and wrote the draft of manuscript with support from Yang KK; Yang KK and Wang YZ proposed the project and gave critical comments of the manuscript; Huang ZC and Zheng E provided some additional suggestions on the experiments; Xiao WX and Li B checked and approved the manuscript. All authors discussed the results.

Conflict of interest The authors declare that they have no conflict of interest.

Supplementary information Experimental details and supporting data are available in the online version of the paper.

Cheng-Jie Fan received his BSc (2014) from Sichuan University, and he is currently a PhD candidate in polymer chemistry and physics under the supervision of Professor Ke-Ke Yang at Sichuan University. His reasearch interest focuses on the robust self-healing polymers.

Ke-Ke Yang received her BSc degree in polymer materials (1994), MSc degree in chemical fiber (1997), and PhD degree in material science from Sichuan University in China. She joined Sichuan University in 1997, and now is a full professor in polymer chemistry and physics. Her research focuses on biodegradable polymers, polymer composites, shape-memory polymers and self-healing materials.

一种高强高韧自修复聚氨酯弹性体：通过多重氢键及其堆积作用实现微相结构的精确调控

范诚杰, 黄子纯, 李蓓, 肖文霞, 郑恩, 杨科珂*, 王玉忠

摘要 自修复材料具有优异的使用安全性、更长的寿命、节能和对环境更低的影响等优势, 因此受到研究者高度关注. 超分子相互作用以其优异的可逆性和对环境刺激的快速响应性, 在自修复材料中得到广泛应用. 但如何通过合理的分子结构设计获得兼具优异机械性能和自修复能力的高分子材料仍是研究者面临的巨大挑战. 本文通过将脲基嘧啶酮(UPy)基团引入到聚丙二醇(PPG)链段中, 并精确调控其微相结构, 得到了一种强韧的可自修复聚氨酯弹性体PPG-mUPy. 聚合物链段中的UPy基团通过二聚形成四重氢键, 不仅可以诱导相分离从而形成软硬段结构, 还可通过π-π堆积相互作用, 在环境温度下形成稳定的微晶, 进一步提高聚氨酯材料的机械强度. 此外, 柔性PPG链段上氨基甲酸酯基团之间存在的弱氢键, 赋予了材料超韧特性. 通过温度调控启动微晶熔融, 释放UPy的可逆特性, 赋予材料优异的自修复性能. 通过调控PPG链段长度、各组分含量及微观形态, 得到综合性能最优样品PPG_{1000}-$mUPy^{50\%}$, 其拉伸强度可达20.62 MPa, 强度修复效率可达93%. 该方法为开发高强高韧自修复高分子材料提供了新的思路.

